

Primary Dielectric-Constant Gas Thermometry in the Range from 2.4 K to 26 K at PTB

C. Gaiser · B. Fellmuth · N. Haft

Published online: 8 January 2008
© Springer Science+Business Media, LLC 2007

Abstract New dielectric-constant gas-thermometry (DCGT) measurements were performed at PTB from 2.4 K to 26 K in order to establish a temperature scale with reduced uncertainty. The progress concerning the measurement of capacitance changes, temperature, and pressure compared with the results published in 1996 is described. This is the first step on the way to determine the Boltzmann constant at the triple point of water. At more than 20 temperatures, isotherms were measured and evaluated performing both single- and multi-isotherm fits. Based on this evaluation, a more accurate DCGT scale has been established that is compared with the constant-volume gas-thermometry scale NPL-75, being one basis of the International Temperature Scale of 1990. Coincidence has been found within only a few tenths of a millikelvin above 3.3 K. This gives, together with literature data, confidence with respect to thermodynamic temperature at this level. Emphasis is also given to the results obtained for the virial coefficients, especially below 3.3 K, where the 1996 DCGT results show strong deviations from the expected behavior. The new experimental data for the second virial coefficient are compared with ab initio calculations.

Keywords Helium · Low temperatures · Primary thermometry · Virial coefficients

1 Introduction

In 1996 [1], PTB published their first dielectric-constant gas-thermometry (DCGT) scale in the range from 4.2 K to 27.0 K. These results were until now the most accurate measurements obtained by this method. Below 6 K, the temperature instability of the bath cryostat used was relatively high. This gave one motivation for building up a

C. Gaiser (✉) · B. Fellmuth · N. Haft
Physikalisch-Technische Bundesanstalt, Abbestr. 2-12, 10587 Berlin, Germany
e-mail: christof.gaiser@ptb.de

new DCGT. In this work, new results are presented in the range between 2.4 K and 26 K. Additionally, supported by the better temperature stability, the measurement of pressure and capacitance changes was improved. Isotherms were measured at more than 20 temperatures and the data evaluated by performing both single- and multi-isotherm fits. The established, more accurate, DCGT scale is first compared with the constant-volume gas-thermometry scale NPL-75 [2] of the National Physical Laboratory, UK, being one basis for the International Temperature Scale of 1990, ITS-90 [3]. The NPL-75 has been supported by later measurements as the best thermodynamic reference [4].

The multi-isotherm fits require appropriate expansions for the temperature dependence of the second, $B(T)$, and third, $C(T)$, virial coefficients. Theoretically predicted expansions were applied yielding stable results for $B(T)$. On the basis of new calculations [5] for the second density $B(T)$ and dielectric $b(T)$ virial coefficients [6], the new experimental data are compared with ab initio values. The agreement concerning $B(T)$ is excellent although it strongly depends on the temperature dependence of the third virial coefficient. At temperatures below 3.3 K, the results obtained suggest a change in the properties of the measuring gas ^4He , i.e., a transition from a real quantum gas, which can be described by a virial expansion, to a gas affected by bosonic interactions.

Together with literature data, coincidence between the new DCGT scale and the NPL-75 within only a few tenths of a millikelvin gives confidence in thermodynamic temperatures above 3.3 K at this level. These results corroborate the DCGT value for the triple-point temperature of hydrogen based on the first DCGT scale of PTB (13.80365(50) K at the deuterium content of $35 \mu\text{mol/mol}$ of the PTB hydrogen sample, which yields 13.8039 K for the recently prescribed SLAP (Standard Light Antarctic Precipitation) deuterium concentration of about $89 \mu\text{mol/mol}$). The uncertainty of the DCGT scale at low temperatures and the good agreement with the ab initio theory for $B(T)$ are the first steps toward a future DCGT experiment at the triple point of water. This experiment will be directed to a new determination of the Boltzmann constant, k , as one basis for a new definition of the base unit of temperature, the kelvin.

2 Measurements

2.1 Theory

2.1.1 DCGT Principle

The basic idea of DCGT [7] is to replace the density in the equation of state of a gas with the dielectric constant, ε , and to measure it by incorporating a capacitor in the gas bulb. The dielectric constant of an ideal gas is given by the relation $\varepsilon = \varepsilon_0 + \alpha_0 N/V$, where ε_0 is the exactly known electric constant, α_0 is the static electric dipole polarizability of the atoms, and N/V is the number density, i.e., the equation of state of an ideal gas can be written in the form $p = kT(\varepsilon - \varepsilon_0)/\alpha_0$. Absolute DCGT requires knowledge of α_0 with the necessary accuracy. Nowadays this condition is fulfilled for helium. Recent progress has decreased the uncertainty of the ab initio value of α_0 well below

one part in 10^6 [8,9]. The molar polarizability A_ε is defined as $A_\varepsilon = N_A \alpha_0 / (3\varepsilon_0)$, i.e., the Boltzmann constant is related to α_0 , A_ε , and the molar gas constant R by

$$k = \frac{R}{A_\varepsilon} \frac{\alpha_0}{3\varepsilon_0} \quad (1)$$

The measurement of the ratio A_ε/R of two macroscopic quantities allows, therefore, the determination of k .

For a real gas, the interaction between the particles has to be considered by combining the virial expansions of the equation of state and the Clausius–Mossotti equation. Neglecting higher order terms and the third dielectric virial coefficient, this yields

$$p \approx \frac{\chi}{\frac{3A_\varepsilon}{RT} + \kappa_{\text{eff}}} \left[1 + \frac{B^*(T)}{3A_\varepsilon} \chi + \frac{C(T)}{(3A_\varepsilon)^2} \chi^2 + \dots \right], \quad (2)$$

where $\chi = \varepsilon/\varepsilon_0 - 1$ is the dielectric susceptibility, $B^*(T) = B(T) - b(T)$, $B(T)$, and $C(T)$ are the second and third density virial coefficients taking into account the pair and triplet interactions, respectively, $b(T)$ is the second dielectric virial coefficient, and κ_{eff} is the effective compressibility of a capacitor used to measure the susceptibility χ . To determine $3A_\varepsilon/RT$, isotherms have to be measured, i.e., the relative change in capacitance, $(C_M(p) - C_M(0))/C_M(0) = \chi + (\varepsilon/\varepsilon_0)\kappa_{\text{eff}} p$ of the gas-filled measuring capacitor is determined as a function of the pressure p of the gas. The capacitance $C_M(p)$ of the capacitor is measured with the space between its electrodes filled with the gas at various pressures and with the space evacuated so that $p=0$ Pa. A polynomial fit to the resulting p versus $(C_M(p) - C_M(0))/C_M(0)$ data points, together with knowledge of the pressure dependence of the dimensions of the capacitor (effective compressibility κ_{eff}), yields $3A_\varepsilon/RT$. Since the susceptibilities of gases are very small, they cannot be determined via absolute capacitance measurements. Even the required measurement of the relative capacitance changes to an uncertainty of a few parts in 10^9 places extreme demands on the parameters of the audio-frequency capacitance bridge.

2.1.2 Theory for the Virial Coefficients of ^4He

To perform the multi-isotherm fits (see Sect. 3.1), analytic expressions for the temperature dependence of the second and third density virial coefficients $B(T)$ and $C(T)$ of the measuring gas ^4He are needed. In the past, many different expressions were used. For the range between 2.6 K and 300 K, Steur et al. [10] deduced for $B(T)$:

$$B_{\text{Steur}}(T) = b_1 T^{-0.25} + b_2 T^{-0.75} + b_3 T^{-1.25} + b_4 T^{-2.5} \\ + b_5 T^{-3.5} + b_6 T^{-6.45} + b_7 T^2, \quad (3)$$

and for $C(T)$:

$$C_{\text{Steur}}(T) = c_1 + c_2 T^{-1} + c_3 T^{-7}. \quad (4)$$

In Eq. 3, the terms with the coefficients b_4 to b_6 were derived by Colclough [11], who calculated the quantum corrections. The other terms were empirically determined. The term with b_7 was introduced by Steur to describe the high-temperature behavior of $B(T)$, i.e., the use of this term in the temperature range presented here has to be discussed (see Sect. 3.1). For $C(T)$, the theoretical predictions are very sparse. A fundamental article by Pais and Uhlenbeck [12] suggests the following form:

$$C_{\text{Pais}}(T) = c_1 + c_2 T^{-1.5} + c_3 T^{-2} + c_4 T^{-3}, \quad (5)$$

although, at that time, the authors did not recommend the use of their expression for comparison with the experiment.

Complete theoretically based analytical expressions for the virial coefficients are unavailable at present. On the other hand, there are different numerical calculations using semi-empirical or ab initio inter-atomic potentials to deduce $B(T)$ [5, 13, 14]. The second dielectric virial coefficient $b(T)$, which is at least 100 times smaller than $B(T)$, was neglected in the past [15]. This was reasonable because the agreement between theoretical and experimental data for $B(T)$ was inadequate. In [5], the uncertainty of the theory for $B(T)$ reached the point where the possible influence of $b(T)$ might consider the theoretical calculations [6], although the scatter of the literature data is substantial (below 30 K, half an order of magnitude) [6, 16].

2.2 Experiment

2.2.1 Cryostat

The cryostat used for the new DCGT is a tank cryostat with a liquid nitrogen and liquid helium tank located in an outer vacuum chamber. The measurement system containing the capacitors is situated in an inner vacuum chamber together with two independent helium-cooling stages. The new design allows temperatures down to 2.4 K to be stabilized for long periods of time (at least 1 day) at a level of some 0.01 mK. Thus, a whole isotherm can be measured under undisturbed thermal conditions. Even at the lowest temperature, no exchange gas is necessary in the inner vacuum chamber to improve the thermal contact between the cooling stages and the measurement system, as was the case for the former bath cryostat used in [1]. Consequently, the temperature stability was improved by at least a factor of two over the whole working range.

2.2.2 Pressure Measurement

Over the whole pressure range, the pressure measurement utilized a commercial piston gauge with an effective area of the piston-cylinder assembly of about 3 cm^2 . The calibration of the effective area A_{eff} is traceable to the national pressure standard of the PTB (relative standard uncertainty of five parts in 10^6). The stability of the piston gauge was checked by cross-float comparisons with a system of the same type. These improvements resulted in an uncertainty reduced by a factor of two compared with the equipment used in [1]. In addition, a new control system for the piston gauge was

built, so that it is possible to stabilize the piston at a certain height for hours. This makes long-term measurements possible.

2.2.3 Measurement of Capacitance Changes

In the new setup, two identical cylindrical capacitors located in the measurement system were used. This leads to a more symmetric setup compared to [1], where the reference capacitor was stabilized at room temperature. Further improvements concern the parasitic impedances of the capacitance bridge, its resolution, and the data acquisition. Now, averaging over long periods of time (30 min per data point) is possible. In combination with the good pressure stability, these improvements have reduced the uncertainty of the measurement of capacitance changes by a factor of two compared with the former DCGT system.

2.2.4 Temperature Measurements

Temperature measurements were performed with a group of rhodium–iron resistance thermometers (RIRTs), the resistances of which were measured by a low-current ac bridge. The calibration of the bridge is traceable to the national standard of PTB (relative uncertainty of two parts in 10^7 of full scale). The RIRTs carry a copy of the NPL-75. The standard uncertainty of coincidence of this PTB copy with that maintained at the NPL amounts to 0.15 mK, which has been estimated on the basis of several comparisons.

2.2.5 Data

In the range between 5 K and 26 K, isotherms were taken at temperatures differing by one kelvin. Below 5 K, the intervals were reduced (temperatures of the isotherms: 2.42 K, 2.5 K, 3.3 K, 4 K, and 4.5 K). For one isotherm, measurements at seven pressures were usually performed. In the liquid-helium temperature range, the maximum pressure was near the condensation pressure of ^4He . However, for the multi-isotherm fit, only data up to half the condensation pressure were used. With 227 triplets of pressure, temperature, and dielectric constant, the amount of data is comparable to that in [1].

3 Results

3.1 Multi-isotherm Fits—DCGT Scale

To decrease the uncertainty of the isotherm fit, a linear least squares fit with orthogonal functions [17] of all measured isotherms is recommended. This so-called multi-isotherm fit decreases the uncertainty because the ratio of the number of data points to the number of fitting parameters is increased. Multi-isotherm fitting requires analytical expressions for $B^*(T)$ and $C(T)$ of Eq. 2. Due to the fact that $b(T)$ is very small, it should be possible to include its temperature dependence in the expansion

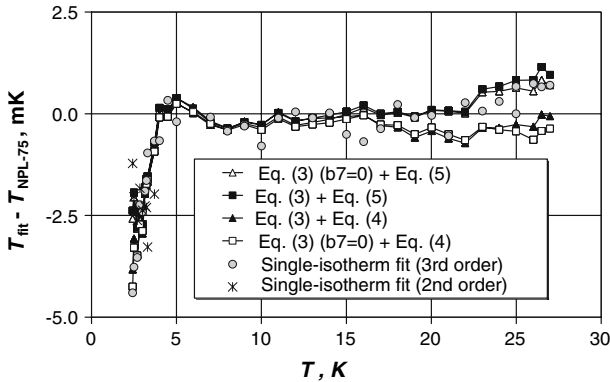


Fig. 1 Deviation of temperature values T_{fit} corresponding to different DCGT fits from NPL-75: Δ : $B^*(T)$ given by Eq. 3 without the quadratic term ($b_7=0$) and $C(T)$ defined by Eq. 5. \blacksquare : as for Δ , but with $b_7 \neq 0$. \blacktriangle : $B^*(T)$ by Eq. 3 with $b_7 \neq 0$ and $C(T)$ by Eq. 4. \square : as for \blacktriangle , but with $b_7 = 0$. \circ : single-isotherm fits done with a third-order series according to Eq. 2. \times : as for \circ , but with a second-order series

corresponding to Eq. 3. In Fig. 1, the results of multi-isotherm fits are shown for different expressions as well as the recently determined value of the effective compressibility κ_{eff} of $1.95 \times 10^{-12} \text{ Pa}^{-1}$. (The κ_{eff} value, with the temperature equivalents of its uncertainty given in Table 1, was determined following the method explained in detail in [1]. For this purpose, five isotherms measured at the triple point of argon were evaluated.) In each case, the difference between the DCGT temperature and the PTB copy of the NPL-75 is plotted. As in [15], Eqs. 3 and 4 suggested by Steur et al. [10] were applied with and without the high-temperature term $b_7 T^2$. In addition, the expression $C_{\text{Pais}}(T)$ proposed by Pais and Uhlenbeck [12] (Eq. 5) for $C(T)$ has been tested. The DCGT temperatures resulting from single-isotherm fits made with a conventional third-order expansion according to Eq. 2 and with a second-order expansion (only for the low-temperature data, see Sect. 3.3), respectively, are also shown in the plot. (The complete equations used for the fits are given in [1].) Below 20 K, the dependence of the DCGT temperature scale on the expressions for $B^*(T)$ and $C(T)$ is obviously marginal. Above 20 K, significant differences exist. The results of the fit with $C_{\text{Pais}}(T)$ follow those of the third-order single-isotherm fits, which is not the case for the fits with $C_{\text{Steur}}(T)$ (Eq. 4). These results and others discussed below led to the decision that $C_{\text{Pais}}(T)$ is the best available analytical expression for the temperature dependence of the third density virial coefficient. Therefore, the results obtained with this expression together with Eq. 3 ($b_7 = 0$) are selected as the new 2007 DCGT scale.

The uncertainty estimates of the different components leading to an uncertainty budget for the new DCGT data are collected in Table 1. The standard uncertainties for the multi-isotherm fits of Fig. 1 increase from 0.13 mK at 2.4 K to 0.40 mK at 26 K. The main uncertainty components result from the measurement of capacitance changes and pressure, the temperature instability, the effective compressibility, the spread of the results of multi-isotherm fits using different adequate expressions $B^*(T)$ and $C(T)$, and the influence of impurities and surface layers (cf. the detailed discussion of the components given in [1]). Leaving aside the change in the dielectric properties of ^4He below 3.3 K, see Sect. 3.3, temperature values deduced from third-order

Table 1 Uncertainty budget for three temperature values resulting from a multi-isotherm fit to the DCGT data (the uncertainty estimates for the different expansions $B(T)$ and $C(T)$ discussed in Sect. 2.1.2 are practically the same, i.e., only one budget is necessary for each temperature)

Component	2.4 K	12 K	26 K
<i>Monte-Carlo simulations (type A components)^a</i>			
Susceptibility	0.03	0.07	0.14
Pressure repeatability	0.03	0.02	0.03
Temperature instability	0.02	0.03	0.06
⁴ He layers	0.12	0.15	0.19
Effective compressibility	0.01	0.03	0.16
<i>Type B estimates^b</i>			
Pressure (A_{eff})	0.01	0.06	0.13
Impurity layers	0.01	0.02	0.04
Impurities in the gas	0.01	0.04	0.07
Combined standard uncertainty	0.13	0.19	0.33
<i>Influence of the expansions for the virial coefficients (type B component, rectangular distribution)^c</i>			
Expansions	0.01	0.03	0.23
Complete combined standard uncertainty	0.13	0.19	0.40

The estimates are given in mK

^a These uncertainties are based on Monte-Carlo simulations performed with one hundred data sets randomized with the standard deviation of the specific quantity

^b These uncertainties are based on calibrations and comparisons of piston gauges for determining the effective area A_{eff} (see Sect. 2.2.2), on literature data for the typical thickness of impurity layers on the capacitor plates, and analysis data (mass spectroscopy) for impurity concentrations in the measuring gas

^c This uncertainty component considers the deviations between the results obtained for the different expansions for the virial coefficients $B(T)$ and $C(T)$, see Eqs. 3–5

single-isotherm fits have a standard uncertainty ranging from 0.24 mK at 2.4 K to 0.57 mK at 26 K. The second-order single-isotherm fit yields at 2.4 K an uncertainty of 0.14 mK, which is comparable to that of the multi-isotherm fits.

In Fig. 2, the new data are compared with the former results given in [1] and [15], which represent different evaluations of the data set upon which the 1996 DCGT scale of PTB is based. (In [1] (best fits 1996), a power series of $(1/T)$ of fifth order is used for $B^*(T)$ together with Eq. 4. To check the influence of $B^*(T)$, Eqs. 3 and 4 were applied in [15] (best fits 2004)). All scale differences are well within the combined standard uncertainties, although below 8 K and above 15 K, the discrepancies are of the order of 0.5 mK. The reason for this might be the improved temperature stability, which results in more reliable data, especially for the upper and lower limits of the temperature range. Near the triple-point temperature of hydrogen, the 1996 and 2007 DCGT scales are in very good coincidence. Thus, the new results corroborate the DCGT value for this triple-point temperature of 13.80365 K at a deuterium content of 35 $\mu\text{mol/mol}$, with a standard uncertainty of 0.5 mK, based on the 1996 DCGT scale [4]. The results corroborate also the thermodynamic accuracy of the NPL-75 scale with a standard uncertainty increasing from 0.3 mK at 4 K to 0.5 mK at 26 K. This standard uncertainty combines that of the DCGT data, see Table 1, and the uncertainty of coincidence of the PTB copy of the NPL-75 with the copy maintained at the NPL, see Sect. 2.2.4.

Concerning the choice of the expression for $C(T)$, the extrapolation behavior of the fitted function $p(\chi)$ at the low-temperature end is a good indication. In Fig. 3,

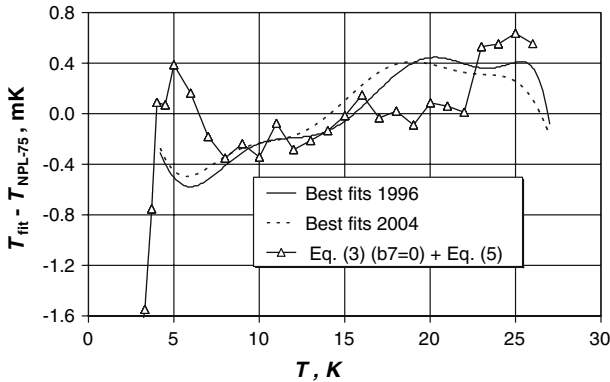


Fig. 2 Deviation of T_{fit} corresponding to different DCGT fits from the NPL-75: Δ : $B^*(T)$ given by Eq. 3 without the quadratic term ($b_7 = 0$) and $C(T)$ defined by Eq. 5. *Solid line*: average of the best fits published in 1996 [1]. *Dotted line*: average of the best fits published in [15] (re-evaluation of the 1996 data)

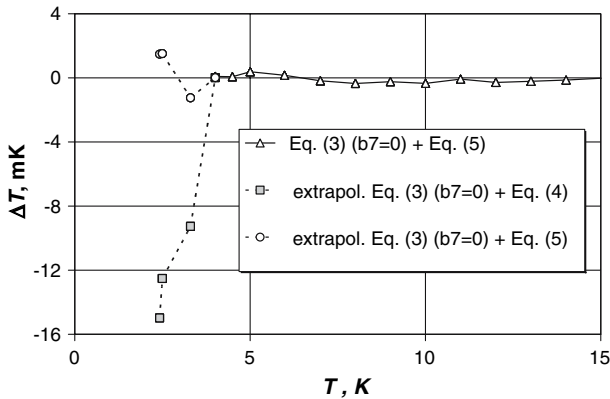


Fig. 3 Differences ΔT between temperatures T_{extr} extrapolated from 4 K downward and those corresponding to NPL-75. \blacksquare : T_{extr} deduced from a fit to data between 4 K and 26 K with $B^*(T)$ by Eq. 3 ($b_7 = 0$) and $C(T)$ by Eq. 4. \circ : T_{extr} deduced as for \blacksquare , but using Eq. 5. Δ : deviation of the full-range-fit temperatures from NPL-75 for comparison purposes

the extrapolated DCGT temperatures of two multi-isotherm fits made with a reduced data set from 4 K to 26 K are compared with the NPL-75. It is obvious that a fit with $C_{\text{Pais}}(T)$ gives an extrapolated temperature that is about a factor of 10 closer to NPL-75 than that of a fit with $C_{\text{Steur}}(T)$. The extrapolation behavior underpins, therefore, the choice of the expression $C_{\text{Pais}}(T)$.

3.2 Second Virial Coefficients $B(T)$ and $b(T)$

In evaluating the quality of the experimental data and the resulting temperature dependences $B^*(T)$ and $C(T)$, theoretical calculations of the second density virial coefficient, part of the leading term in the virial expansion, are of crucial importance.

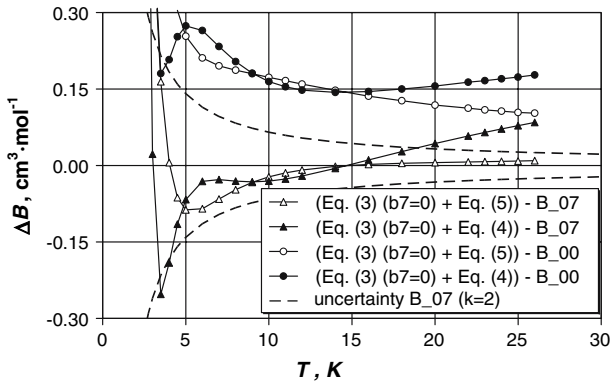


Fig. 4 Differences ΔB between different $B^*(T)$ values determined by multi-isotherm fits and the ab initio results B_{00} [13] and B_{07} [5], respectively. Δ : $B^*(T) - B_{07}$ ($B^*(T)$ deduced from a fit using $B^*(T)$ given by Eq. 3 with $b_7 = 0$ and $C(T)$ defined by Eq. 5). \circ : as previous, but compared with B_{00} . \blacktriangle : $B^*(T) - B_{07}$ ($B^*(T)$ based on Eqs. 3 and 4). \bullet : as previous, but compared with B_{00} . Dashed lines give the expanded uncertainties of B_{07} for a coverage factor of two. (Symbols do not represent experimental data points, but are only added for a better marking of the different curves)

A recalculation [5] of $B(T)$ data first published in 2000 [13] makes it possible to compare the new DCGT results with ab initio values at an unprecedented level of uncertainty. In Fig. 4, the differences between $B^*(T)$ results of multi-isotherm fits performed with $C_{\text{Pais}}(T)$ and $C_{\text{Steur}}(T)$, and the two sets of ab initio values, are shown. In comparing the results with the old ab initio calculation [13], both fitting results are in much better agreement with the new theoretical values. Especially evident for temperatures above 20 K, the $B^*(T)$ DCGT results obtained using $C_{\text{Steur}}(T)$ are not in accordance with the theory. Also, oscillations are observable which suggest that the polynomial $C_{\text{Steur}}(T)$ is not optimal. By contrast, the fit with $C_{\text{Pais}}(T)$ yields smooth behavior over the whole temperature interval, and the accordance with the ab initio data is impressive, especially in the range above 10 K. The standard uncertainty of these $B^*(T)$ data decreases from $0.26 \text{ cm}^3 \cdot \text{mol}^{-1}$ at 2.4 K to $0.03 \text{ cm}^3 \cdot \text{mol}^{-1}$ at 5 K and amounts to about $0.02 \text{ cm}^3 \cdot \text{mol}^{-1}$ above 10 K.

Up to now, the second density virial coefficient was assumed to be the dominant term in the virial expansion and the second dielectric virial coefficient $b(T)$ was considered negligible. In fact, recent quantum statistical calculations for $b(T)$ [6] concluded that $b(T)$ is smaller than formerly predicted by the semi-classical calculations of the same group [18] and the ab initio calculations by [16]. Nevertheless, the small deviation of the DCGT $B^*(T)$ results from the improved theory for $B(T)$ is at the level where $b(T)$ has to be taken into account. In Fig. 5, the DCGT $B^*(T)$ results obtained with $C_{\text{Pais}}(T)$ are compared with the new ab initio data for $B(T)$ as in Fig. 4, but additional theoretical estimates for $B^*(T) = B(T) - b(T)$ are considered. Furthermore, results for the 1996 DCGT data set (DCGT1) are added. The influence of $b(T)$ is comparable to the claimed uncertainty of the theory only at higher temperatures. There, the coincidence with theory is significantly better for the 2007 DCGT results (DCGT2).

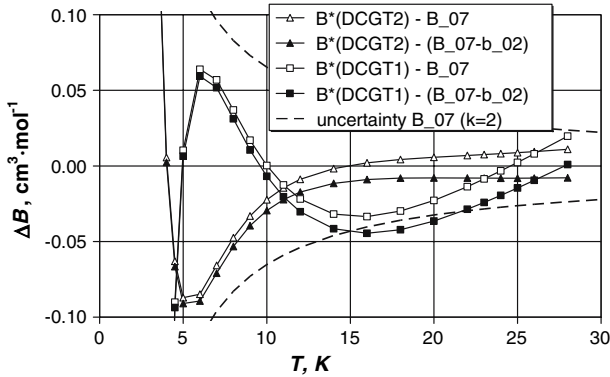


Fig. 5 Comparison of experimental virial coefficients $B^*(T)$ (DCGT1 [1] and DCGT2 the present work) with ab initio results B_{07} [5] and b_{02} [6] for the second density and dielectric virial coefficients, respectively. All multi-isotherm fits were performed with $B^*(T)$ given by Eq. 3 with $b_7 = 0$ and $C(T)$ defined by Eq. 5. Δ : $B^*(T) - B_{07}$ for DCGT2. \blacktriangle : as previous, but $B^*(T)$ compared with $B_{07} - b_{02}$. \square : $B^*(T) - B_{07}$ for DCGT1. \blacksquare : as previous, but compared with $B_{07} - b_{02}$. Dashed lines give the expanded uncertainties of B_{07} for a coverage factor of two. (Symbols do not represent experimental data points, but are only added for a better marking of the different curves)

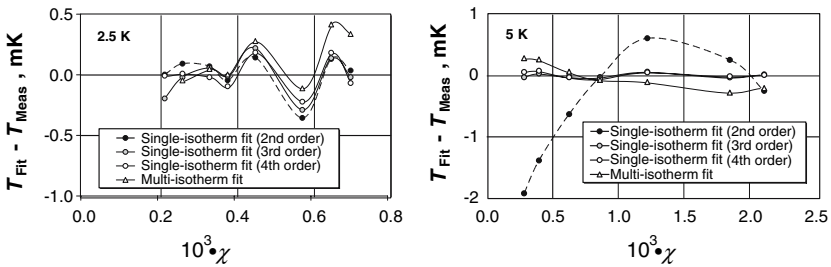


Fig. 6 On the left: fit residuals (temperature equivalent of the deviation of experimental data $p_i(\chi_i)$ from the fit function $p(\chi)$) for the 2.5 K isotherm data and different single-isotherm fits as well as the multi-isotherm fit according to Eq. 3 with $b_7 = 0$ and Eq. 5. On the right: corresponding fit residuals for the 5 K isotherm

3.3 Effects Below 3.3 K

A closer look at the low-temperature part of Fig. 1 shows that the multi- and single-isotherm-fit results deviate strongly from the NPL-75 below 3.3 K. To analyze the situation in more detail, it is instructive to look at the fit residuals (deviation of the experimental data $p_i(\chi_i)$ from the fit function $p(\chi)$) obtained for single-isotherm fits of different order. In Fig. 6, the temperature equivalents of these fit residuals are shown for 2.5 K and 5 K.

At 5 K, it is evident that, the second fit order is not able to describe the isotherm. The plotted differences are of order 1 mK in contrast to the third- and fourth-order fits, for which the residuals approach 0.05 mK. In addition, the multi-isotherm-fit residuals display larger differences than the third- and fourth-order fits, due to the larger number of data points (227) compared to the fit order, but these differences

are also much smaller than those for the second-order fit. This behavior shows that higher orders of the virial expansion become important at the higher gas densities of ^4He at low temperatures, i.e., the third and fourth virial coefficients are not negligible. At 2.5 K, the situation changes dramatically. The second-order fit function is able to describe the whole isotherm about as well as the higher-order functions. The following results are further evidence of a special situation below 3.3 K (further details are given in Ref. [19]):

- The single-isotherm fits of different orders yield temperature values which differ by up to several mK from each other, whereas the second-order fit values are closest to NPL-75.
- The results for the virial coefficients obtained from the single-isotherm fits do not coincide with theoretical and experimental literature data. For the third virial coefficient, they are also not in accordance with the results of the multi-isotherm fit. The deviations are larger for the higher fit orders.
Thus, the data obtained for ^4He below 3.3 K cannot be described by a virial expansion. It must of course be verified that this unexpected result is not influenced by deficiencies of the DCGT method at low temperatures. Three facts are of special importance:
- As Yang and Lee [20] deduced in their work, the virial expansion is not valid near phase transitions. Since the data considered here were obtained up to half the condensation pressure, a transition to the liquid phase could be excluded.
- Also, new experiments concerning ^4He films on gold [21] (the measuring capacitor is gold-plated) show that there are at most a few monolayers on the electrodes at a temperature of 2.34 K and in the pressure range used here. Therefore, the existence of ^4He films does not explain the unexpected behavior.
- Isotherm measurements at 2.47 K and 3.23 K using ^3He were performed and analyzed. Further details are given in Ref. [19]. The results can be well described by a virial expansion. The isotherm temperatures coincide with the NPL-75 copy within 0.1 mK, and the values for the second and third virial coefficients agree well with literature data. This proves the feasibility of DCGT even at very low temperatures.

Since the classical constant-volume gas-thermometry data for ^4He [2] do not show peculiarities below 3.3 K, the sudden change in the ^4He gas properties mainly concerns the dielectric parameters. This might be caused by the formation of clusters due to the attractive bosonic interaction of the ^4He atoms. For small spherical dielectric clusters, it can be shown [22] that the polarizability is enhanced and decreases slightly to the value corresponding to the atomic polarizability with increasing cluster size. If the polarizability of ^4He clusters deviates from that which results from the ab initio value for the ^4He atoms, the DCGT temperatures deduced using the ab initio value will of course be wrong, as is the case below 3.3 K. Furthermore, the special bosonic interaction might cause a large second dielectric virial coefficient. Then, the dependence of the pressure p on the dielectric susceptibility χ (and thus on the ^4He gas density) may be approximated by the linear and quadratic terms in the expansion $p(\chi)$, i.e., second-order single-isotherm fits yield a good approximation. Finally, an additional non-polynomial term connected with the special interaction can make other

fit functions necessary and thus higher-order polynomial fits will not help, but will increase the uncertainty of the fit results. For a detailed discussion, see [19].

4 Conclusions

A new DCGT temperature scale has been established using an experimental setup with improved parameters compared with the former setup described in [1]. Evaluating a large data set of 227 triplets of pressure, temperature, and dielectric constant, a reduced standard uncertainty of the scale ranging from 0.15 mK at 4 K to 0.4 mK at 26 K has been achieved. For the data evaluation by multi-isotherm fits, it was necessary to select appropriate expressions for the temperature dependence of the second ($B(T)$) and third virial coefficients ($C(T)$) of the measuring gas ^4He . A theoretically-based expansion for $C(T)$ yielded the most stable results. The differences between the obtained $B(T)$ results and new ab initio values are well within the uncertainty estimates above 3.3 K, which confirms the quality of both the DCGT data and its evaluation. The comparison of the results with literature data corroborates the thermodynamic accuracy of the NPL-75 scale, being one basis for the ITS-90, with a combined standard uncertainty increasing from 0.3 mK at 4 K to 0.5 mK at 26 K. It corroborates also the value for the triple-point temperature of hydrogen of 13.80365(50) K at a deuterium content of 35 $\mu\text{mol/mol}$ [4] that is based on the 1996 DCGT data set [1]. This value yields a triple-point temperature of 13.8039 K for the recently prescribed SLAP (Standard Light Antarctic Precipitation) deuterium concentration of about 89 $\mu\text{mol/mol}$. All these results support the potential of the DCGT method to determine the Boltzmann constant at the triple point of water within the claimed uncertainty [23] as a basis for the new definition of the base unit of temperature, the kelvin [24].

Below 3.3 K, a drastic change in the pressure versus dielectric susceptibility (and thus density) characteristics of ^4He gas was found. This might be interpreted as a transition of the real quantum gas from the behavior which can be described by a virial expansion to a behavior dominated by a special bosonic attractive interaction causing clustering of the ^4He atoms. This special behavior seems to be characterized by a pressure versus dielectric susceptibility dependence of first and second order and a modified molar polarizability.

References

1. H. Luther, K. Grohmann, B. Fellmuth, *Metrologia* **33**, 341 (1996)
2. K.H. Berry, *Metrologia* **15**, 89 (1979)
3. H. Preston-Thomas, *Metrologia* **27**, 3 (1990)
4. R.L. Rusby, M.R. Moldover, J. Fischer, D.R. White, P.P.M. Steur, R.P. Hudson, M. Durieux, K.D. Hill, *Working Documents of the 23rd Meeting of the Consultative Committee for Thermometry*, BIPM, document CCT/05-19 (2005)
5. J.J. Hurly, J.B. Mehl, *J. Res. Natl. Inst. Stand. Technol.* **112**, 75 (2007)
6. A. Rizzo, C. Hättig, B. Fernández, H. Koch, *J. Chem. Phys.* **117**, 2609 (2002)
7. D. Gogan, G.W. Michel, *Metrologia* **16**, 149 (1980)
8. W. Cencek, K. Szalewicz, B. Jeziorski, *Phys. Rev. Lett.* **86**, 5675 (2001)
9. G. Lach, B. Jeziorski, K. Szalewicz, *Phys. Rev. Lett.* **92**, 233001 (2004)
10. P.P.M. Steur, M. Durieux, G.T. McConville, *Metrologia* **24**, 69 (1987)

11. A.R. Colclough, *Metrologia* **15**, 183 (1979)
12. A. Pais, G.E. Uhlenbeck, *Phys. Rev.* **116**, 250 (1959)
13. J.J. Hurly, M.R. Moldover, *J. Res. Natl. Inst. Stand. Technol.* **105**, 667 (2000)
14. R.A. Aziz, M.J. Slaman, *Metrologia* **27**, 211(1990)
15. B. Fellmuth, J. Fischer, C. Gaiser, N. Haft, in *Proceedings of TEMPMEKO 2004, 9th International Symposium on Temperature and Thermal Measurements in Industry and Science*, ed. by D. Zvizdić, L.G. Bermanec, T. Veliki, T. Stašić (FSB/LPM, Zagreb, Croatia, 2004), pp. 73–78
16. R. Moszynski, T.G.A. Heijmen, P.E.S. Wormer, A. van der Avoird, *J. Chem. Phys.* **104**, 6997 (1996)
17. K.R. Hall, F.B. Canfield, *Physica* **33**, 481 (1967)
18. H. Koch, C. Hättig, H. Larsen, J. Olsen, P. Jørgensen, B. Fernández, A. Rizzo, *J. Chem. Phys.* **111**, 10108 (1999)
19. C. Gaiser, B. Fellmuth, submitted to *Phys. Rev. Lett.*
20. C.N. Yang, T.D. Lee, *Phys. Rev.* **87**, 404 (1952)
21. T. McMillan, J.E. Rutledge, P. Taborek, *J. Low Temp. Phys.* **138**, 995 (2005)
22. H.Y. Kim, J.O. Sofo, D. Velegol, M.W. Cole, G. Mukhopadhyay, *Phys. Rev. A* **72**, 053201 (2005)
23. B. Fellmuth, Ch. Gaiser, J. Fischer, *Meas. Sci. Technol.* **17**, R145 (2006)
24. I.M. Mills, P.J. Mohr, T.J. Quinn, B.N. Taylor, E.R. Williams, *Metrologia* **43**, 227 (2006)